Personalized Schedules for Prostate Cancer Biopsies

Anirudh Tomer[1],*, Daan Nieboer[2], Monique J. Roobol[3],

Ewout W. Steyerberg[2], and Dimitris Rizopoulos[1]

[1]Department of Biostatistics, Erasmus University Medical Center, the Netherlands

[2]Department of Public Health, Erasmus University Medical Center, the Netherlands

[3]Department of Urology, Erasmus University Medical Center, the Netherlands

*email: atomer@erasmusmc.nl

SUMMARY: Low risk prostate cancer patients enrolled in active surveillance (AS) programs have to undergo biopsies on a frequent basis for examination of disease progression. Majority of the AS programs worldwide employ fixed schedules of biopsies for all patients. It has been found that such fixed and frequent schedules discourage patients to receive biopsies, and also bring a financial burden on the healthcare systems. Motivated by the world's largest AS program PRIAS, in this paper we present personalized schedules for biopsies to counter these problems. Using joint models for time to event and longitudinal data, our methods combine information from previous biopsy results and historical prostate-specific antigen (PSA) levels of a patient, to schedule the next biopsy. We also present criteria to compare the efficacy of personalized schedules with that of existing biopsy schedules, and a method to select the optimal schedule.

KEY WORDS: Active surveillance; Joint models; Personalized medicine; Prostate cancer;.

This paper has been submitted for consideration for publication in *Biometrics*

1. Introduction

In this decade prostate cancer is the second most frequently diagnosed cancer (14% of all cancers) in males worldwide, with nearly 67% of all prostate cancer cases reported in developed countries (Torre et al., 2015). The increase in diagnosis of low grade prostate cancers has been attributed to increase in life expectancy and increase in number of screening programs (Potosky et al., 1995). A major issue of screening programs that also has been established in other types of cancers (e.g., breast cancer) is over-diagnosis. To avoid overtreatment, patients diagnosed with low grade prostate cancer are often motivated to join active surveillance (AS) programs. The goal of AS is to routinely examine the progression of prostate cancer and avoid serious treatments such as surgery or chemotherapy as long as they are not needed.

Currently the largest AS program worldwide is Prostate Cancer Research International Active Surveillance, also known as PRIAS (Bokhorst et al., 2016). Patients enrolled in PRIAS are closely monitored using serum prostate-specific antigen (PSA) levels, digital rectal examination (DRE) and repeat prostate biopsies. Results from biopsies are graded on a scale called Gleason, which takes values between 2 and 10, with 10 corresponding to a serious state of the disease. At the time of induction in PRIAS, patients must have a Gleason score of six or less, DRE score of cT2c or less and a PSA of 10 ng/mL or less. In PRIAS, a PSA doubling time (PSA-DT) of less than three years indicates prostate cancer progression, where PSA-DT is measured as the inverse of the slope of regression line through the base two logarithm of PSA values. However until either DRE or Gleason are observed to be higher than the aforementioned thresholds, patients are not removed from AS for curative treatment (Bokhorst et al., 2016). When the Gleason score becomes greater than six, it is also known as Gleason reclassification (referred to as GR hereafter).

Biopsies are reliable but they are also difficult to conduct, cause pain and have serious side effects such as hematuria and sepsis (Loeb et al., 2013). Due to these reasons, majority

of the AS programs worldwide strongly advise at most one biopsy per year. Conducting a biopsy annually (we refer to it as annual schedule hereafter) has the advantage that GR can be detected within one year of its occurrence. This may work well for patients with a faster progressing disease, however for patients with a slower progressing disease many unnecessary biopsies are scheduled. The drawbacks of unnecessary biopsies are not only medical but also financial. Keegan et al. (2012) have shown that annual schedules can cost more than the treatment (brachytherapy or prostatectomy) to AS programs, and if biopsies were to be conducted every other year, then up to 28% increase in savings per head from AS over treatment could be achieved. Despite this, several AS programs employ the annual schedule (Tosoian et al., 2011; Welty et al., 2015).

Scheduling frequent biopsies for patients has also lead to a high non-compliance rate for repeat biopsies (Bokhorst et al., 2015), which reduces the effectiveness of AS programs because progression is detected late. In PRIAS some of the reasons reported for non-compliance were: 'patient does not want biopsy', 'complications on last biopsy' and 'no signs of disease progression on previous biopsy'. The PRIAS schedule and the compliance rates are: one biopsy each at year one (81%), year four (60%), year seven (53%) and year 10 (33%). After year 10 biopsies are conducted every five years. An exception is made, if at any time a patient has PSA-DT less than 10 years, wherein the annual schedule is prescribed. It is important to note that, unlike biopsies, measurement of PSA has a high compliance rate of 91% in PRIAS. This is because PSA is easy to obtain and measuring PSA does not lead to any side effects. The use of PSA-DT in the scheduling process is justified, because it was found to be indicative of GR in PRIAS (Bokhorst et al., 2015).

This paper is motivated by the need to reduce the burden of biopsies and most optimally find the onset of GR. To this end, we intend to create personalized schedules for biopsies which improve upon the PRIAS and annual schedule. That is, a different schedule for every

patient utilizing his recorded information. Personalized schedules for screening have received much interest in the literature, especially in the medical decision making context. For diabetic retinopathy, cost optimized personalized schedules based on Markov models have been developed by Bebu and Lachin (2017). For breast cancer, personalized mammography screening policy based on the prior screening history and personal risk characteristics of women, using partially observable Markov decision process (MDP) models have been proposed by Ayer, Alagoz, and Stout (2012). MDP models have also been used to develop personalized screening policies for cervical cancer (Akhavan-Tabatabaei, Sánchez, and Yeung, 2017) and colorectal cancer (Erenay, Alagoz, and Said, 2014). Another type of model called joint model for time to event and longitudinal data (Tsiatis and Davidian, 2004; Rizopoulos, 2012) has also been used to create personalized schedules, albeit for longitudinal biomarkers (Rizopoulos et al., 2016). In context of prostate cancer, Zhang et al. (2012) have used partially observable MDP models to personalize the decision of (not) deferring a biopsy to the next checkup time during the screening process. The decision is based on the baseline characteristics as well as a discretized PSA level of the patient at the current check up time.

Our work differs from the above referenced work in certain aspects. Firstly, the schedules we propose in this paper, account for the latent between-patient heterogeneity. We achieve this using joint models, which are inherently patient-specific because they utilize random effects. Secondly, joint models allow a continuous time scale and utilize the entire history of PSA levels. Lastly, instead of making a binary decision of (not) deferring a biopsy to the next check up time, we schedule biopsies at a per patient optimal future time, utilizing the historical PSA measurements and repeat biopsy results of the patient up to the current check up time. To this end, using joint models we first obtain a full specification of the joint distribution of PSA levels and time of GR. We then use it to define a patient-specific posterior predictive distribution of the time of GR given the observed PSA measurements and previous

biopsies. Using the general framework of Bayesian decision theory, we propose a set of loss functions which are minimized to find the optimal time of conducting a biopsy. These loss functions yield us two categories of personalized schedules, those based on expected time of GR and those based on the risk of GR. We also analyze an approach where the two types of schedules are combined. To compare the proposed personalized schedules with the PRIAS and annual schedule we conduct a simulation study, and then discuss various criteria for evaluating the efficacy of each schedule, and a method to choose the most suitable one.

The rest of the paper is organized as follows. Section 2 briefly covers the joint modeling framework. Section 3 details the personalized scheduling approaches we have proposed in this paper. In Section 4 we discuss criteria for evaluation of the efficacy of a schedule and the choice of the optimal schedule. In Section 5 we demonstrate the personalized schedules by employing them for the patients from the PRIAS program. Lastly, in Section 6, we present the results from a simulation study we conducted to compare personalized schedules with PRIAS and annual schedule.

2. Joint Model for Time to Event and Longitudinal Outcomes

We start with the definition of the joint modeling framework that will be used to fit a model to the available dataset, and then to plan biopsies for future patients. Let T_i^* denote the true GR time for the i-th patient enrolled in an AS program. Let the vector of times at which biopsies are conducted for this patient be denoted by $T_i^b = \{T_{i0}^b, T_{i1}^b, \ldots, T_{iN_i^b}^b; T_{ij}^b < T_{ik}^b, \forall j < k\}$, where N_i^b are the total number of biopsies conducted. Because of the periodical nature of biopsy schedules, T_i^* cannot be observed directly and it is only known to fall in an interval $(l_i, r_i]$, where $l_i = T_{iN_i^b-1}^b, r_i = T_{iN_i^b}^b$ if GR is observed, and $l_i = T_{iN_i^b}^b, r_i = \infty$ if patient drops out of AS before GR is observed. Further let $\boldsymbol{y}_i$ denote the $n_i \times 1$ vector of PSA levels for the i-th patient. For a sample of n patients the observed data is denoted by $\mathcal{D}_n = \{l_i, r_i, \boldsymbol{y}_i; i = 1, \ldots, n\}$.

The longitudinal outcome of interest, namely PSA level is continuous in nature and thus to model it the joint model utilizes a linear mixed effects model (LMM) of the form:

$$y_i(t) = m_i(t) + \varepsilon_i(t)$$

$$= \boldsymbol{x}_i^T(t)\boldsymbol{\beta} + \boldsymbol{z}_i^T(t)\boldsymbol{b}_i + \varepsilon_i(t),$$

where $\boldsymbol{x}_i(t)$ denotes the row vector of the design matrix for fixed effects and $\boldsymbol{z}_i(t)$ denotes the same for random effects. Correspondingly the fixed effects are denoted by $\boldsymbol{\beta}$ and random effects by $\boldsymbol{b}_i$. The random effects are assumed to be normally distributed with mean zero and $q \times q$ covariance matrix $\boldsymbol{D}$. The true and unobserved PSA level at time t is denoted by $m_i(t)$. Unlike $y_i(t)$, the former is not contaminated with the measurement error $\varepsilon_i(t)$. The error is assumed to be normally distributed with mean zero and variance σ^2, and is independent of the random effects $\boldsymbol{b}_i$.

To model the effect of PSA on hazard of GR, joint models utilize a relative risk sub-model. The hazard of GR for patient i at any time point t, denoted by $h_i(t)$, depends on a function of subject specific linear predictor $m_i(t)$ and/or the random effects:

$$h_i(t \mid \mathcal{M}_i(t), \boldsymbol{w}_i) = \lim_{\Delta t \to 0} \frac{\Pr\{T_i^* \epsilon [t, t + \Delta t) \mid T_i^* \geqslant t, \mathcal{M}_i(t), \boldsymbol{w}_i\}}{\Delta t}$$

$$= h_0(t) \exp\left[\boldsymbol{\gamma}^T \boldsymbol{w}_i + f\{M_i(t), \boldsymbol{b}_i, \boldsymbol{\alpha}\}\right], \quad t > 0,$$

where $\mathcal{M}_i(t) = \{m_i(v), 0 \leqslant v \leqslant t\}$ denotes the history of the underlying PSA levels up to time t. The vector of baseline covariates is denoted by $\boldsymbol{w}_i$, and $\boldsymbol{\gamma}$ are the corresponding parameters. The function $f(\cdot)$ parametrized by vector $\boldsymbol{\alpha}$ specifies the functional form of PSA levels (Brown, 2009; Rizopoulos, 2012; Taylor et al., 2013; Rizopoulos et al., 2014) that is used in the linear predictor of the relative risk model. Some functional forms relevant to the problem at hand are the following:

$$\begin{cases} f\{M_i(t), \boldsymbol{b}_i, \boldsymbol{\alpha}\} = \alpha m_i(t), \\ f\{M_i(t), \boldsymbol{b}_i, \boldsymbol{\alpha}\} = \alpha_1 m_i(t) + \alpha_2 m_i'(t), \quad \text{with } m_i'(t) = \frac{\mathrm{d}m_i(t)}{\mathrm{d}t}. \end{cases}$$

These formulations of $f(\cdot)$ postulate that the hazard of GR at time t may be associated

with the underlying level $m_i(t)$ of the PSA at t, or with both the level and velocity $m_i'(t)$ of the PSA at t. Lastly, $h_0(t)$ is the baseline hazard at time t, and is modeled flexibly using P-splines. More specifically:

$$\log h_0(t) = \gamma_{h_0,0} + \sum_{q=1}^{Q} \gamma_{h_0,q} B_q(t, \boldsymbol{v}),$$

where $B_q(t, \boldsymbol{v})$ denotes the q-th basis function of a B-spline with knots $\boldsymbol{v} = v_1, \dots, v_Q$ and vector of spline coefficients γ_{h_0}. To avoid choosing the number and position of knots in the spline, a relatively high number of knots (e.g., 15 to 20) are chosen and the corresponding B-spline regression coefficients γ_{h_0} are penalized using a differences penalty (Eilers and Marx, 1996).

For the estimation of joint model's parameters we use a Bayesian approach. The details of the estimation method are presented in Web Appendix A of the supplementary material.

3. Personalized Schedules for Repeat Biopsies

Once a joint model for GR and PSA levels is obtained, the next step is to use it to create personalized schedules for biopsies. Let us assume that a personalized schedule is to be created for a new patient j, who is not present in the original sample $\mathcal{D}_n$ of patients. Further let us assume that this patient did not have a GR at his last biopsy performed at time t, and that the PSA levels are available up to a time point s. The goal is to find the optimal time $u > \max(t, s)$ of the next biopsy.

3.1 *Posterior Predictive Distribution for Time to GR*

Let $\mathcal{Y}_j(s)$ denote the history of PSA levels taken up to time s for patient j. The information from PSA history and repeat biopsies is manifested by the posterior predictive distribution $g(T_j^*)$, given by (conditioning on baseline covariates $\boldsymbol{w}_i$ is dropped for notational simplicity

hereafter):

$$g(T_j^*) = p\{T_j^* \mid T_j^* > t, \mathcal{Y}_j(s), \mathcal{D}_n\}$$

$$= \int p\{T_j^* \mid T_j^* > t, \mathcal{Y}_j(s), \boldsymbol{\theta}\} p(\boldsymbol{\theta} \mid \mathcal{D}_n) \mathrm{d}\boldsymbol{\theta}$$

$$= \int \int p\{T_j^* \mid T_j^* > t, \boldsymbol{b_j}, \boldsymbol{\theta}\} p\{\boldsymbol{b_j} \mid T_j^* > t, \mathcal{Y}_j(s), \boldsymbol{\theta}\} p(\boldsymbol{\theta} \mid \mathcal{D}_n) \mathrm{d}\boldsymbol{b_j} \mathrm{d}\boldsymbol{\theta}. \quad (1)$$

The distribution $g(T_j^*)$ depends on the observed longitudinal history of patient j via the random effects $\boldsymbol{b_j}$, and on the information from the original dataset $\mathcal{D}_n$ via the posterior distribution of the parameters $p(\boldsymbol{\theta} \mid \mathcal{D}_n)$, where $\boldsymbol{\theta}$ denotes the vector of all parameters.

3.2 *Loss Functions*

To find the time u of the next biopsy, we use principles from statistical decision theory in a Bayesian setting (Berger, 1985; Robert, 2007). More specifically, we propose to choose u by minimizing the posterior expected loss $E_g\{L(T_j^*, u)\}$, where the expectation is taken with respect to $g(T_j^*)$. The former is given by:

$$E_g\{L(T_j^*, u)\} = \int_t^\infty L(T_j^*, u) p\{T_j^* \mid T_j^* > t, \mathcal{Y}_j(s), \mathcal{D}_n\} \mathrm{d}T_j^*.$$

Various loss functions $L(T_j^*, u)$ have been proposed in literature (Robert, 2007). The ones we utilize, and the corresponding motivations are presented next.

One of the reasons, patients did not comply with the existing PRIAS schedule was 'complications on a previous biopsy'. Therefore, it is required to have as less biopsies as possible. In the ideal case only one biopsy, performed at the exact time of GR is sufficient. Hence, neither a time which overshoots the true GR time T_j^*, nor a time which undershoots is preferred. In this regard, the squared loss function $L(T_j^*, u) = (T_j^* - u)^2$ and absolute loss function $L(T_j^*, u) = |T_j^* - u|$ have the properties that the posterior expected loss is symmetric on both sides of T_j^*. Secondly, both loss functions have well known solutions available. The

posterior expected loss for the squared loss function is given by:

$$E_g\{L(T_j^*, u)\} = E_g\{(T_j^* - u)^2\}$$

$$= E_g\{(T_j^*)^2\} + u^2 - 2uE_g(T_j^*). \tag{2}$$

The posterior expected loss in (2) attains its minimum at $u = E_g(T_j^*)$, the expected time of GR. The posterior expected loss for the absolute loss function is given by:

$$E_g\{L(T_j^*, u)\} = E_g(|T_j^* - u|)$$

$$= \int_u^\infty (T_j^* - u)g(T_j^*)\mathrm{d}T_j^* + \int_t^u (u - T_j^*)g(T_j^*)\mathrm{d}T_j^*. \tag{3}$$

The posterior expected loss in (3) attains its minimum at the median of $g(T_j^*)$, given by $u = \pi_j^{-1}(0.5 \mid t, s)$, where $\pi_j^{-1}(\cdot)$ is the inverse of dynamic survival probability $\pi_j(u \mid t, s)$ of patient j (Rizopoulos, 2011). It is given by:

$$\pi_j(u \mid t, s) = \Pr\{T_j^* \geqslant u \mid T_j^* > t, \mathcal{Y}_j(s), D_n\}, \quad u \geqslant t. \tag{4}$$

For ease of readability we denote $\pi_j^{-1}(0.5 \mid t, s)$ as $\mathrm{median}(T_j^*)$ hereafter.

Even though the mean or median time of GR may be obvious choices from a statistical perspective, from the viewpoint of doctors or patients, it could be more intuitive to make the decision for the next biopsy by placing a cutoff $1 - \kappa, \kappa\epsilon[0, 1]$ on the risk of GR. This approach would be successful if κ can sufficiently well differentiate between patients who will obtain GR in a given period of time, and those who will not. This approach is also useful when patients are apprehensive about delaying biopsies beyond a certain risk cutoff. In this regard, a biopsy can be scheduled at a time point u such that the dynamic risk of GR is higher than a certain threshold $1 - \kappa$, beyond u. To this end, the posterior expected loss for the following multilinear loss function can be minimized to find the optimal u:

$$L_{k_1,k_2}(T_j^*, u) = \begin{cases} k_2(T_j^* - u), k_2 > 0 & \text{if } T_j^* > u, \\ k_1(u - T_j^*), k_1 > 0 & \text{otherwise.} \end{cases} \tag{5}$$

where k_1, k_2 are constants parameterizing the loss function. The posterior expected loss

$E_g\{L_{k_1,k_2}(T_j^*, u)\}$ obtains its minimum at $u = \pi_j^{-1}\{k_1/(k_1 + k_2) \mid t, s\}$ (Robert, 2007). The choice of the two constants k_1 and k_2 is equivalent to the choice of $\kappa = k_1/(k_1 + k_2)$.

3.2.1 *A Hybrid Approach.* In practice, for some patients we may not have sufficient information, resulting in high variance of $g(T_j)$, which in turn would make using a measure of central tendency such as mean or median time of GR unreliable (i.e., overshooting the true T_j^* by a big margin). In such occasions, the approach based on dynamic risk of GR could be more robust. This consideration leads us to a hybrid approach, namely, to select u using dynamic risk of GR based approach when the spread of $g(T_j^*)$ is large, while using $E_g(T_j^*)$ or median(T_j^*) when the spread of $g(T_j^*)$ is small. What constitutes a large spread will be application-specific. In the PRIAS, within the first 10 years, the maximum possible delay in detection of GR is three years. Thus we propose that if the difference between the 0.025 quantile of $g(T_j^*)$, and $E_g(T_j^*)$ or median(T_j^*) is more than three years then proposals based on dynamic risk of GR be used instead.

3.3 *Estimation*

Since there is no closed form solution available for $E_g(T_j^*)$, for its estimation we utilize the following relationship between $E_g(T_j^*)$ and $\pi_j(u \mid t, s)$:

$$E_g(T_j^*) = t + \int_t^\infty \pi_j(u \mid t, s)\mathrm{d}u. \tag{6}$$

There is no closed form solution available for the integral in (6), and hence we approximate it using Gauss-Kronrod quadrature. We preferred this approach over Monte Carlo methods to estimate $E_g(T_j^*)$ from $g(T_j^*)$, because sampling directly from $g(T_j^*)$ involved an additional step of sampling from the distribution $p(T_j^* \mid T_j^* > t, \boldsymbol{b_j}, \boldsymbol{\theta})$, as compared to the estimation of $\pi_j(u \mid t, s)$ (Rizopoulos, 2011). The former approach was thus computationally faster.

As mentioned earlier, selection of the optimal biopsy time based on $E_g(T_j^*)$ alone will not

be practically useful when the $\text{var}_g(T_j^*)$ is large, which is given by:

$$\text{var}_g(T_j^*) = 2 \int_t^\infty (u - t)\pi_j(u \mid t, s)\mathrm{d}u - \left\{ \int_t^\infty \pi_j(u \mid t, s)\mathrm{d}u \right\}^2. \tag{7}$$

Since a closed form solution is not available for the variance expression, it is estimated similar to the estimation of $E_g(T_j^*)$. The variance depends both on last biopsy time t and PSA history $\mathcal{Y}_j(s)$. The impact of the observed information on variance is demonstrated in Section 5.2.

For schedules based on dynamic risk of GR, the value of κ dictates the biopsy schedule and thus its choice has important consequences. In certain cases it may be chosen on the basis of doctor's advice or the amount of risk that is acceptable to the patient. For example, if the maximum acceptable risk is 75%, then $\kappa = 0.25$.

In cases where κ cannot be chosen on the basis of the input of the physician or the patients, we propose to automate the choice of κ. More specifically, we propose to choose a κ for which a binary classification accuracy measure (López-Ratón et al., 2014), discriminating between cases and controls, is maximized. In PRIAS, cases are patients who experience GR and the rest are controls. However, a patient can be in control group at some time t and in the cases at some future time point $t + \Delta t$, and thus time dependent binary classification is more relevant. In joint models, a patient j is predicted to be a case if $\pi_j(t + \Delta t \mid t, s) \leqslant \kappa$ and a control if $\pi_j(t + \Delta t \mid t, s) > \kappa$ (Rizopoulos, 2016; Rizopoulos, Molenberghs, and Lesaffre, 2017). The time window Δt can be automatically chosen as $\arg\max_{\Delta t} \text{AUC}(t, \Delta t, s)$, the latter being a measure of discriminative capability of the model (Rizopoulos, 2016; Rizopoulos et al., 2017). However such a time window may not be clinically relevant at all. In AS programs at any point in time, it is of interest to identify patients who may obtain GR in the next one year from those who do not, so that they can be provided immediate attention (in exceptional cases a biopsy within an year of the last one). Thus, in this work we use a Δt of one year.

For automatic selection of the threshold κ, we require a binary classification accuracy

measure which is in line with the goal to focus on patients whose true time of GR falls in the time window Δt. To this end, the measure which combines both sensitivity and precision is F_1 score. It is defined as:

$$F_1(t, \Delta t, s) = 2\frac{\text{TPR}(t, \Delta t, s)\text{PPV}(t, \Delta t, s)}{\text{TPR}(t, \Delta t, s) + \text{PPV}(t, \Delta t, s)}, \quad F_1 \epsilon [0, 1],$$

$$\text{TPR}(t, \Delta t, s) = \text{Pr}\{\pi_j(t + \Delta t \mid t, s) \leqslant \kappa \mid T_j^* \epsilon(t, t + \Delta t]\},$$

$$\text{PPV}(t, \Delta t, s) = \text{Pr}\{T_j^* \epsilon(t, t + \Delta t] \mid \pi_j(t + \Delta t \mid t, s) \leqslant \kappa\}.$$

where $\text{TPR}(\cdot)$ and $\text{PPV}(\cdot)$ denote time dependent true positive rate (sensitivity) and positive predictive value (precision), respectively. The estimation for both is similar to the estimation of $\text{AUC}(t, \Delta t, s)$ given by Rizopoulos et al. (2017). Since a high F_1 score is desired, the optimal value of κ is $\arg\max_\kappa F_1(t, \Delta t, s)$. In this work we compute the latter using a grid search approach. That is, first F_1 is computed using the available dataset over a fine grid of κ values in the interval $[0, 1]$, and then κ corresponding to the highest F_1 is chosen.

3.4 *Algorithm*

The aforementioned personalized schedules, schedule biopsy at a time $u > \max(t, s)$. However, if time $u < T_j^*$, then GR is not detected at u and at least one more biopsy is required at an optimal time $u^{new} > \max(u, s)$. This process is iteratively repeated until GR is detected. To aid in medical decision making, we elucidate this process via an algorithm in Figure 7. Since it is required by PRIAS that biopsies are conducted at a gap of at least one year, when $u - t < 1$, the algorithm postpones u to $t + 1$, because it is the time nearest to u, at which the one year gap condition is satisfied.

[Figure 1 about here.]

4. Choosing a Schedule

Given a particular schedule S of biopsies, our next goal is to evaluate the efficacy of this schedule and to compare it with other schedules. To this end, we first present the criteria for evaluation of efficacy of biopsy schedules and then discuss the choice of the optimal schedule.

4.1 *Evaluation of Efficacy of Schedules*

We measure the efficacy of a schedule S using two criteria, namely, for the j-th patient the number of biopsies $N_j^{bS} \epsilon [1, \infty]$ a schedule conducts before GR is detected, and the offset $O_j^S \epsilon [0, \infty]$ by which it overshoots the true GR time T_j^*. The offset O_j^S is defined as $O_j^S = T_{jN_j^{bS}}^S - T_j^*$, where $T_{jN_j^{bS}}^S \geqslant T_j^*$ is the time at which GR is detected. Our interest lies in the joint distribution $p(N_j^{bS}, O_j^S)$ of the number of biopsies and the offset. Given the medical and financial burden associated with biopsies, ideally only one biopsy which leads to a zero offset should be conducted. That is, a method with a low mean number of biopsies $E(N_j^{bS})$ as well a low mean offset $E(O_j^S)$ is desired. It is also desired that a method has low variance of the number of biopsies $\text{var}(N_j^{bS})$, as well as low variance of the offset $\text{var}(O_j^S)$, so that the method works similarly for most patients. Quantiles of $p(N_j^{bS})$ may also be of interest. For example, a schedule which conducts less than two biopsies in 95% of the cases may be preferred.

4.2 *Finding the Optimal Schedule*

Given the multiple measures of efficacy of a schedule, the next step is to find the optimal schedule. Using principles from compound optimal designs (Läuter, 1976) we propose to choose a schedule S which minimizes a loss function of the following form:

$$L(S) = \sum_{r=1}^{R} \eta_r \mathcal{R}_r(N_j^{bS}). \tag{8}$$

where $\mathcal{R}_r(\cdot)$ is a measure of efficacy of either the number of biopsies or the offset (in the equation above, only N_j^{bS} is used for brevity of notation). Some examples of $\mathcal{R}_r(\cdot)$ are mean,

median, variance and quantile function. Constants $\eta_1, \ldots, \eta_R$, where $\eta_r \epsilon [0, 1]$ and $\sum_{r=1}^{R} \eta_r = 1$, are weights to differentially weigh-in the contribution of each of the R measures of efficacy. An example loss function is:

$$L(S) = \eta_1 E(N_j^{bS}) + \eta_2 E(O_j^S). \tag{9}$$

The choice of η_1 and η_2 is not easy, because biopsies have serious medical side effects and consequently the cost of an extra biopsy cannot be quantified or compared to a unit increase in offset easily. To obviate this problem we utilize the equivalence between compound and constrained optimal designs (Cook and Wong, 1994). More specifically, it can be shown that for any η_1 and η_2 there exists a constant $C > 0$ for which minimization of loss function in (9) is equivalent to minimization of the loss function subject to the constraint that $E(O_j^S) < C$. That is, the optimal schedule is the one with the least number of biopsies and an offset less than C. The choice of C now can be based on the protocol of AS program. In the more generic case in (8), the optimal solution can be found by minimizing $\mathcal{R}_R(\cdot)$ under the constraint $\mathcal{R}_r(\cdot) < C_r; r = 1, \ldots, R - 1$.

5. Personalized Schedules for Patients in PRIAS

To demonstrate how the personalized schedules work, we apply them to the patients enrolled in PRIAS. To this end, we divide the PRIAS dataset into a training dataset with 5264 patients and a demonstration dataset with three patients who never experienced GR. We fit a joint model to the training dataset and then use it to create personalized schedules for patients in demonstration dataset. We fit the joint model using the R package JMbayes (Rizopoulos, 2016), which uses the Bayesian methodology to estimate the model parameters.

5.1 *Fitting the Joint Model to PRIAS Dataset*

The training dataset contains age at the time of induction in PRIAS, PSA levels and the time interval in which GR is detected, for 5264 prostate cancer patients. PSA was measured

at every three months for first two years and every six months thereafter. To detect GR, biopsies were conducted as per the PRIAS schedule (Section 1). For the longitudinal analysis of PSA we use $\log_2$ PSA measurements instead of the raw data. This because the PSA scores take very large values around the time of disease progression, indicating that the underlying distribution for PSA is right skewed. The longitudinal sub-model of the joint model we fit is given by:

$$\log_2 \text{PSA}(t) = \beta_0 + \beta_1(Age - 70) + \beta_2(Age - 70)^2 + \sum_{k=1}^{4} \beta_{k+2} B_k(t, \mathcal{K})$$
$$+ b_{i0} + b_{i1} B_7(t, 0.1) + b_{i2} B_8(t, 0.1) + \varepsilon_i(t). \tag{10}$$

where $B_k(t, \mathcal{K})$ denotes the k-th basis function of a B-spline with three internal knots at $\mathcal{K} = \{0.1, 0.5, 4\}$ years, and boundary knots at zero and seven years. The spline for the random effects consists of one internal knot at 0.1 years and boundary knots at zero and seven years. The choice of knots was based on exploratory analysis as well as on model selection criteria AIC and BIC. Age of patients was median centered to avoid numerical instabilities during parameter estimation. For the relative risk sub-model the hazard function we fit is given by:

$$h_i(t) = h_0(t) \exp \left\{ \gamma_1(Age - 70) + \gamma_2(Age - 70)^2 + \alpha_1 m_i(t) + \alpha_2 m_i'(t) \right\}. \tag{11}$$

where α_1 and α_2 are measures of strength of the association between hazard of GR and $\log_2$ PSA value $m_i(t)$ and $\log_2$ PSA velocity $m_i'(t)$, respectively. Since the PRIAS schedule depends only on the observed PSA values (via PSA-DT), the interval censoring observed in PRIAS is independent and non informative of the underlying health of the patient.

From the joint model fitted to the PRIAS dataset we found that only $\log_2$ PSA velocity was strongly associated with hazard of GR. For any patient, a unit increase in $\log_2$ PSA velocity led to an 11 times increase in the hazard of GR. The parameter estimates for the fitted joint model are presented in detail in Web Appendix C of the supplementary material.

5.2 *Demonstration of Personalized Schedules*

Using the demonstration dataset, we next present the functioning of personalized schedules based on expected time of GR and dynamic risk of GR. The first patient of interest is patient 3174. The evolution of PSA, repeat biopsy history and proposed times of biopsies for this patient are shown in the top panel of Figure 2. It can be seen that the schedule of biopsy based on expected time of GR adjusts the times of biopsy according to the rise in hazard, which increases due steep rise in $\log_2$ PSA velocity. More specifically, at year two the proposed biopsy time is 12.5 years whereas at year four it decreases to 5.3 years. On average, a biopsy scheduled using expected time of GR at year two should have a larger offset O_j^S compared to the same at year four. This is because the standard deviation of $g(T_j^*)$, given by $\mathrm{SD}_g(T_j^*) = \sqrt{\mathrm{var}_g(T_j^*)}$, is considerably lower at year four as shown in the bottom panel of Figure 2. In the figure it can be seen that the standard deviation also strongly depends on $\log_2$ PSA velocity. As for the schedules based on dynamic risk of GR, the optimal $1 - \kappa$ value was found to be between 0 and 0.1 at all time points, because of the sharp rise in PSA values. This value of κ corresponds to a time very close to the time of latest biopsy ($t = 0$). Hence the biopsies are scheduled much earlier than those based on expected time of GR.

[Figure 2 about here.]

The demonstration of personalized schedules for the two other patients from the demonstration data set is discussed in Web Appendix D of the supplementary material.

6. Simulation Study

The application of personalized schedules for patients from PRIAS demonstrated that the schedules adapt according to the historical data of each patient. However we could not perform a full scale comparison between personalized and PRIAS schedules, because the true time of GR was not known for any of the PRIAS patients. To this end, we have performed

a simulation study comparing personalized schedules with PRIAS and annual schedule, the details of which are presented next.

6.1 *Simulation Setup*

First we assume a population of patients enrolled in AS, with the same entrance criteria as that of PRIAS. The PSA and hazard of GR for patients from this population follows a joint model of the form postulated in Section 5.1, with parameters equal to the posterior mean of parameters (Web Appendix C of the supplementary material) estimated from the joint model fitted to PRIAS dataset. We further assume that there are three equal sized subgroups G_1, G_2 and G_3 of patients in the population, differing in the time of GR. This was done because we wanted to test the efficacy of different schedules for a population with a mixture of patients, namely, those with faster progressing cancer, as well as those with slowly progressing cancer. The time of GR in each subgroup is controlled by a Weibull distributed baseline hazard. The shape and scale parameters (k, λ) of this distribution for the three subgroups are: $(1.5, 4)$, $(3, 5)$ and $(4.5, 6)$ for G_1, G_2 and G_3, respectively. The effect of these parameters is that the variance of time of GR is highest for G_1 and lowest for G_3, while the mean GR time is lowest in G_1 and highest in G_3.

From this population we have sampled 500 datasets with 1000 patients each. Patients are randomly assigned to a subgroup. Further, each dataset is split into a training (750 patients) and a test (250 patients) part. The k-th simulated training dataset $\mathcal{D}^k$ is given by $\mathcal{D}^k = \{l_{ki}, r_{ki}, \boldsymbol{y}_{ki}; i = 1, \ldots, 750\}$, where $\boldsymbol{y}_{ki}$ denote the PSA measurements for the i-th patient in $\mathcal{D}^k$. The frequency of PSA measurements is same as that in PRIAS. Other than simulating a true GR time T^*_{ki}, we also generate a random and non-informative censoring time C_{ki}. When $T^*_{ki} < C_{ki}$, then $l_{ki} = r_{ki} = T^*_{ki}$, otherwise $l_{ki} = C_{ki}$ and $r_{ki} = \infty$. For the test patients, censoring time is not generated.

We next fit a joint model of the specification given in (10) and (11) to each of the $\mathcal{D}^k, k =$

$1, \ldots, 500$, and obtain a MCMC sample from the posterior distribution $p(\boldsymbol{\theta} \mid \mathcal{D}^k)$. We then obtain $g(T_{kl}^*)$ for each of the l-th test patient of the k-th data set and conduct hypothetical biopsies for him. For every patient we conduct biopsies using the following six types of schedules: personalized schedules based on expected time of GR, median time of GR and dynamic risk of GR, and, a hybrid approach between median time of GR and dynamic risk of GR, PRIAS schedule and annual schedule. The biopsies are conducted iteratively in accordance with the algorithm in Figure 7.

To compare the aforementioned schedules we require estimates of the various measures of efficacy of schedules (Section 4). To this end, we compute pooled estimates of each of the $E(N_j^{bS})$, $\text{var}(N_j^{bS})$, $E(O_j^S)$ and $\text{var}(O_j^S)$, as below:

$$\widehat{E(O_j^S)} = \frac{\sum_{k=1}^{500} n_k \widehat{E(O_k^S)}}{\sum_{k=1}^{500} n_k},$$

$$\widehat{\text{var}(O_j^S)} = \frac{\sum_{k=1}^{500} (n_k - 1) \widehat{\text{var}(O_k^S)}}{\sum_{k=1}^{500} (n_k - 1)},$$

where n_k denotes the number of test patients, $\widehat{E(O_k^S)} = \sum_{l=1}^{n_k} O_{kl}^S / n_k$ is the estimated mean and $\widehat{\text{var}(O_k^S)} = \sum_{l=1}^{n_k} \left\{ O_{kl}^S - \widehat{E(O_k^S)} \right\}^2 / (n_k - 1)$ is the estimated variance of the offset for the k-th simulation. The estimates for number of biopsies are obtained similarly.

6.2 *Results*

The pooled estimates of the various measures of efficacy are summarized in Table 1. In addition, mean offset is plotted against mean number of biopsies in Figure 3. From the figure it is evident that across the methods there is an inverse relationship between $E(N_j^{bS})$ and $E(O_j^S)$. For example, the annual schedule conducts 5.2 biopsies on average, which is the highest among all schedules, however it has the least average offset of 6 months as well. On the other hand the schedule based on expected time of GR conducts only 1.9 biopsies on average, the least among all schedules, but it also has the highest average offset of 15 months. The schedule based on median time of GR performs similar to that based on expected time of

GR. Since the annual schedule attempts to contain the offset within an year it has the least $\mathrm{SD}(O_j^S) = \sqrt{\mathrm{var}(O_j^S)}$. However to achieve so, it conducts a wide range of number of biopsies from patient to patient, i.e., highest $\mathrm{SD}(N_j^{bS}) = \sqrt{\mathrm{var}(N_j^{bS})}$. Schedules based on expected and median time of GR perform the opposite of annual schedule in terms of $\mathrm{SD}(N_j^{bS})$ and $\mathrm{SD}(O_j^S)$.

[Figure 3 about here.]

[Table 1 about here.]

The PRIAS schedule conducts only 0.3 biopsies less than annual schedule, but with a higher variance of offset, it does not guarantee early detection for everyone. If we compare the PRIAS schedule with dynamic risk of GR based schedule, we can see that the latter performs better than PRIAS schedule in all aspects. The hybrid approach combines the benefits of methods with low $E(N_j^{bS})$ and $\mathrm{SD}(N_j^{bS})$, and methods with low $E(O_j^S)$ and $\mathrm{SD}(O_j^S)$. It conducts 1.5 less biopsies than annual schedule on average and with a $E(O_j^S)$ of 9.7 months it detects GR within an year since its occurrence. Moreover, it has both $\mathrm{SD}(N_j^{bS})$ and $\mathrm{SD}(O_j^S)$ comparable to PRIAS.

We next discuss the performance of these schedules for each of the 3 subgroups G_1, G_2 and G_3. We observe that annual schedule remains the most consistent across subgroups in terms of the offset, but it varies the most in terms of number of biopsies, conducting 2 extra biopsies in subgroup G_3 (highest mean, low variance of GR time) than in G_1 (low mean, high variance of GR time). The performance of schedule based on expected time of GR is the most consistent in terms of number of biopsies but most inconsistent in terms of offset. It performs the best in subgroup G_3. For the dynamic risk of GR based schedule and the hybrid approach the dynamics are similar to that of the annual schedule. Unlike the latter two schedules, the PRIAS schedule not only conducts more biopsies in G_3 than G_1 but also has a higher offset for G_3 than G_1.

[Figure 4 about here.]

[Figure 5 about here.]

The choice of the optimal schedule using (8) depends on the chosen measures of efficacy. For example, schedule based on dynamic risk of GR is the optimal if on average the least number of biopsies are to be conducted, while simultaneously making sure that at least 90% of the patients have an average offset less than an year (Figure 4 and 5). The schedule based on expected time of GR is optimal if on average the least number of biopsies are to be conducted, while simultaneously making sure that at least 80% of the patients have an average offset less than 2 years. For at least 90% of the patients it detects GR within 3 years, while conducting 2 biopsies on average. We however recommend the hybrid approach, since it conducts only 3.8 biopsies on average while guaranteeing an offset of 24 months for 95% of the patients and 36 months for 99.9% of the patients. Besides if further cutoffs are required on variance of number of biopsies or offset they are not too high either for the hybrid approach.

7. Discussion

In this paper we presented personalized biopsy schedules for patients enrolled in AS programs. The problem at hand was that low risk prostate cancer patients enrolled in AS have to undergo repeat biopsies on a frequent basis for examination of disease progression, which causes medical side effects to patients and also brings financial burden on healthcare systems. Because of these issues, AS programs such as PRIAS are observing a high non-compliance for repeat biopsies, which further increases the chances of delayed detection of disease progression. To approach these problems we proposed personalized schedules based on joint model for time to event and longitudinal data. At any given point in time, the personalized schedules we proposed utilize a patient's information from historical PSA measurements and

repeat biopsies conducted up to that time. We proposed two different classes of personalized schedules for individual patients. They are schedules based on the central tendency of the distribution of time of GR of a patient, and schedules based on dynamic risk of GR. In addition we also proposed a combination (hybrid approach) of these two approaches, which is effective even in scenarios where variance of time of GR for a patient is high. We then proposed criteria for evaluation of various schedules and a method to select the most optimal schedule.

We demonstrated using PRIAS dataset that the personalized schedules adjust the time of biopsy on the basis of results from historical biopsies and PSA, even when the two are not in concordance with each other (Web Appendix D). Secondly, we conducted a simulation study to compare various schedules. We observed that personalized schedules based on dynamic risk of GR performed better than PRIAS schedule in terms of both mean and variance of number of biopsies and offset. We also observed that the PRIAS schedule conducted more biopsies and had higher offset for patients having higher mean GR time. We prefer the schedule based on dynamic risk of GR over PRIAS schedule on the basis of these results. The schedules based on expected and median time of GR conducted only two biopsies on average, which is very promising compared to PRIAS and annual schedule which conducted 4.9 and 5.2 biopsies on average, respectively. In addition, for the former two schedules, at least 90% of the patients had an offset less than 36 months, which is the maximum possible offset in PRIAS during the first 10 years of AS. If a stronger restriction is prescribed for the offset, then we propose that the hybrid approach be used since it neither conducts too many biopsies nor it has a very high offset.

While each of the personalized methods has their own disadvantages and advantages, they also offer multiple choices to the AS programs to choose one as per their requirements, instead of choosing a common fixed schedule for all patients. In this regard, there is potential to

develop more personalized schedules. For example, using loss functions which asymmetrically penalize overshooting/undershooting the target GR time can be interesting. Depending upon the requirements it is also possible to choose κ on the basis of binary classification accuracy measures which focus on non-cases as well (Web Appendix E). Although in this work we assumed that GR time was interval censored, in reality the Gleason scores are susceptible to inter-observer variation (Carlson et al., 1998). Models and schedules which account for error in measurement of time of GR, will be interesting to investigate further. Lastly, there is potential for including diagnostic information from Magnetic resonance imaging (MRI) or DRE. Unlike PSA levels, such information may not always be continuous in nature, in which case our proposed methodology can be very easily extended by utilizing the framework of generalized linear mixed models.

Supplementary Materials

Web Appendix A, C, D and E referenced in Section 2, Section 5, and Section 7, and the derivation of Equation (6) and (7) in Web Appendix B, are available in the document supplementary_material.pdf.

References

Akhavan-Tabatabaei, R., Sánchez, D. M., and Yeung, T. G. (2017). A Markov decision process model for cervical cancer screening policies in colombia. *Medical Decision Making* **37,** 196–211.

Ayer, T., Alagoz, O., and Stout, N. K. (2012). A POMDP approach to personalize mammography screening decisions. *Operations Research* **60,** 1019–1034.

Bebu, I. and Lachin, J. M. (2017). Optimal screening schedules for disease progression with application to diabetic retinopathy. *Biostatistics* doi:`10.1093/biostatistics/kxx009`.

Berger, J. O. (1985). *Statistical Decision Theory and Bayesian Analysis.* Springer Science & Business Media.

Bokhorst, L. P., Alberts, A. R., Rannikko, A., Valdagni, R., Pickles, T., Kakehi, Y., Bangma, C. H., Roobol, M. J., study group PRIAS, et al. (2015). Compliance rates with the Prostate Cancer Research International Active Surveillance (PRIAS) protocol and disease reclassification in noncompliers. *European Urology* **68,** 814–821.

Bokhorst, L. P., Valdagni, R., Rannikko, A., Kakehi, Y., Pickles, T., Bangma, C. H., Roobol, M. J., study group PRIAS, et al. (2016). A decade of active surveillance in the PRIAS study: an update and evaluation of the criteria used to recommend a switch to active treatment. *European Urology* **70,** 954–960.

Brown, E. R. (2009). Assessing the association between trends in a biomarker and risk of event with an application in pediatric HIV/AIDS. *The Annals of Applied Statistics* **3,** 1163–1182.

Carlson, G. D., Calvanese, C. B., Kahane, H., and Epstein, J. I. (1998). Accuracy of biopsy Gleason scores from a large uropathology laboratory: use of a diagnostic protocol to minimize observer variability. *Urology* **51,** 525–529.

Cook, R. D. and Wong, W. K. (1994). On the equivalence of constrained and compound optimal designs. *Journal of the American Statistical Association* **89,** 687–692.

Eilers, P. H. and Marx, B. D. (1996). Flexible smoothing with B-splines and penalties. *Statistical Science* **11,** 89–121.

Erenay, F. S., Alagoz, O., and Said, A. (2014). Optimizing colonoscopy screening for

colorectal cancer prevention and surveillance. *Manufacturing & Service Operations Management* **16,** 381–400.

Keegan, K. A., Dall'Era, M. A., Durbin-Johnson, B., and Evans, C. P. (2012). Active surveillance for prostate cancer compared with immediate treatment. *Cancer* **118,** 3512–3518.

Läuter, E. (1976). Optimal multipurpose designs for regression models. *Mathematische Operationsforschung und Statistik* **7,** 51–68.

Loeb, S., Vellekoop, A., Ahmed, H. U., Catto, J., Emberton, M., Nam, R., Rosario, D. J., Scattoni, V., and Lotan, Y. (2013). Systematic review of complications of prostate biopsy. *European Urology* **64,** 876–892.

López-Ratón, M., Rodríguez-Álvarez, M. X., Cadarso-Suárez, C., Gude-Sampedro, F., et al. (2014). OptimalCutpoints: an R package for selecting optimal cutpoints in diagnostic tests. *Journal of Statistical Software* **61,** 1–36.

Potosky, A. L., Miller, B. A., Albertsen, P. C., and Kramer, B. S. (1995). The role of increasing detection in the rising incidence of prostate cancer. *JAMA* **273,** 548–552.

Rizopoulos, D. (2011). Dynamic predictions and prospective accuracy in joint models for longitudinal and time-to-event data. *Biometrics* **67,** 819–829.

Rizopoulos, D. (2012). *Joint Models for Longitudinal and Time-to-Event Data: With Applications in R.* CRC Press.

Rizopoulos, D. (2016). The R package JMbayes for fitting joint models for longitudinal and time-to-event data using MCMC. *Journal of Statistical Software* **72,** 1–46.

Rizopoulos, D., Hatfield, L. A., Carlin, B. P., and Takkenberg, J. J. (2014). Combining dynamic predictions from joint models for longitudinal and time-to-event data using Bayesian model averaging. *Journal of the American Statistical Association* **109,** 1385–1397.

Rizopoulos, D., Molenberghs, G., and Lesaffre, E. M. (2017). Dynamic predictions with time-dependent covariates in survival analysis using joint modeling and landmarking. *Biometrical Journal* doi:`10.1002/bimj.201600238`.

Rizopoulos, D., Taylor, J. M. G., Van Rosmalen, J., Steyerberg, E. W., and Takkenberg, J. J. M. (2016). Personalized screening intervals for biomarkers using joint models for longitudinal and survival data. *Biostatistics* **17,** 149–164.

Robert, C. (2007). *The Bayesian choice: from decision-theoretic foundations to computational implementation.* Springer Science & Business Media.

Taylor, J. M., Park, Y., Ankerst, D. P., Proust-Lima, C., Williams, S., Kestin, L., Bae, K., Pickles, T., and Sandler, H. (2013). Real-time individual predictions of prostate cancer recurrence using joint models. *Biometrics* **69,** 206–213.

Torre, L. A., Bray, F., Siegel, R. L., Ferlay, J., Lortet-Tieulent, J., and Jemal, A. (2015). Global cancer statistics, 2012. *CA: A Cancer Journal for Clinicians* **65,** 87–108.

Tosoian, J. J., Trock, B. J., Landis, P., Feng, Z., Epstein, J. I., Partin, A. W., Walsh, P. C., and Carter, H. B. (2011). Active surveillance program for prostate cancer: an update of the Johns Hopkins experience. *Journal of Clinical Oncology* **29,** 2185–2190.

Tsiatis, A. A. and Davidian, M. (2004). Joint modeling of longitudinal and time-to-event data: an overview. *Statistica Sinica* **14,** 809–834.

Welty, C. J., Cowan, J. E., Nguyen, H., Shinohara, K., Perez, N., Greene, K. L., Chan, J. M., Meng, M. V., Simko, J. P., Cooperberg, M. R., et al. (2015). Extended followup and risk factors for disease reclassification in a large active surveillance cohort for localized prostate cancer. *The Journal of Urology* **193,** 807–811.

Zhang, J., Denton, B. T., Balasubramanian, H., Shah, N. D., and Inman, B. A. (2012). Optimization of prostate biopsy referral decisions. *Manufacturing & Service Operations Management* **14,** 529–547.
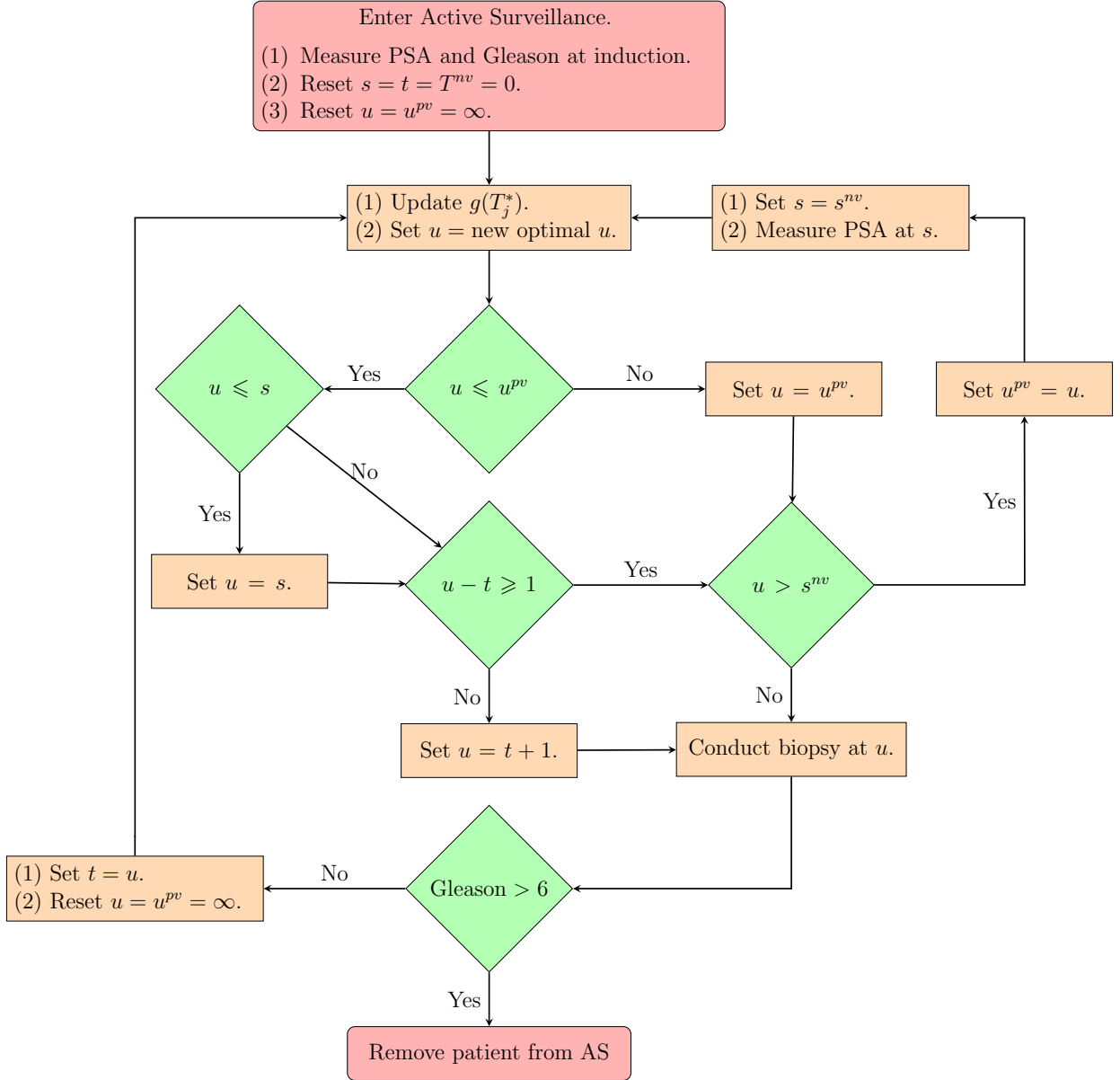
Figure 1. Algorithm for creating a personalized schedule for patient j. The time of the latest biopsy is denoted by t. The time of the latest available PSA measurement is denoted by s. The proposed personalized time of biopsy is denoted by u. The time at which a repeat biopsy was proposed on the last visit to the hospital is denoted by u^{pv}. The time of the next visit for the measurement of PSA is denoted by T^{nv}.
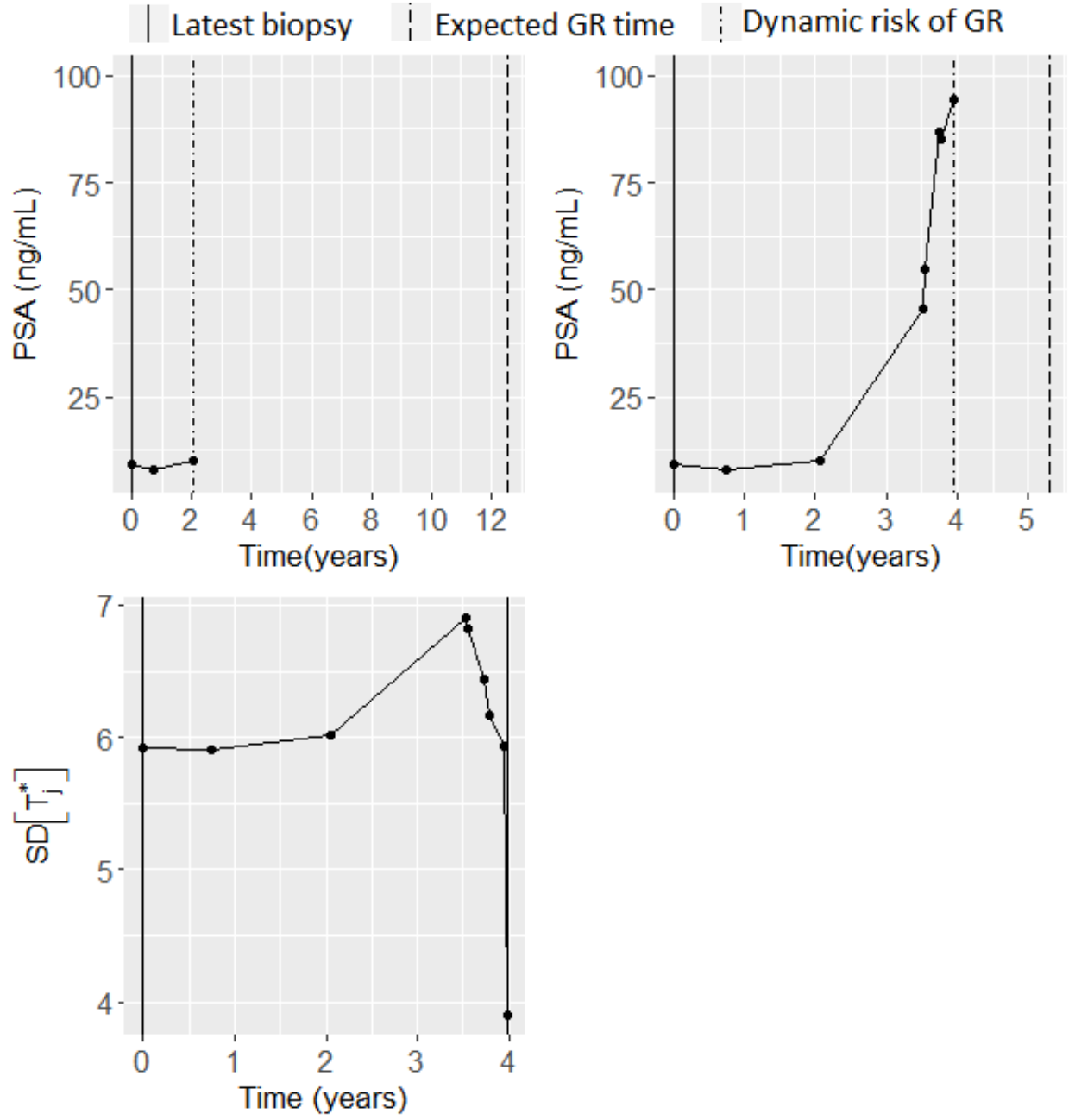
Figure 2. Top panel: Evolution of PSA, history of repeat biopsies and corresponding personalized schedules for patient 3174. Bottom Panel: History of repeat biopsies and $\mathrm{SD}_g(T_j^*) = \sqrt{\mathrm{var}_g(T_j^*)}$ over time for patient 3174.
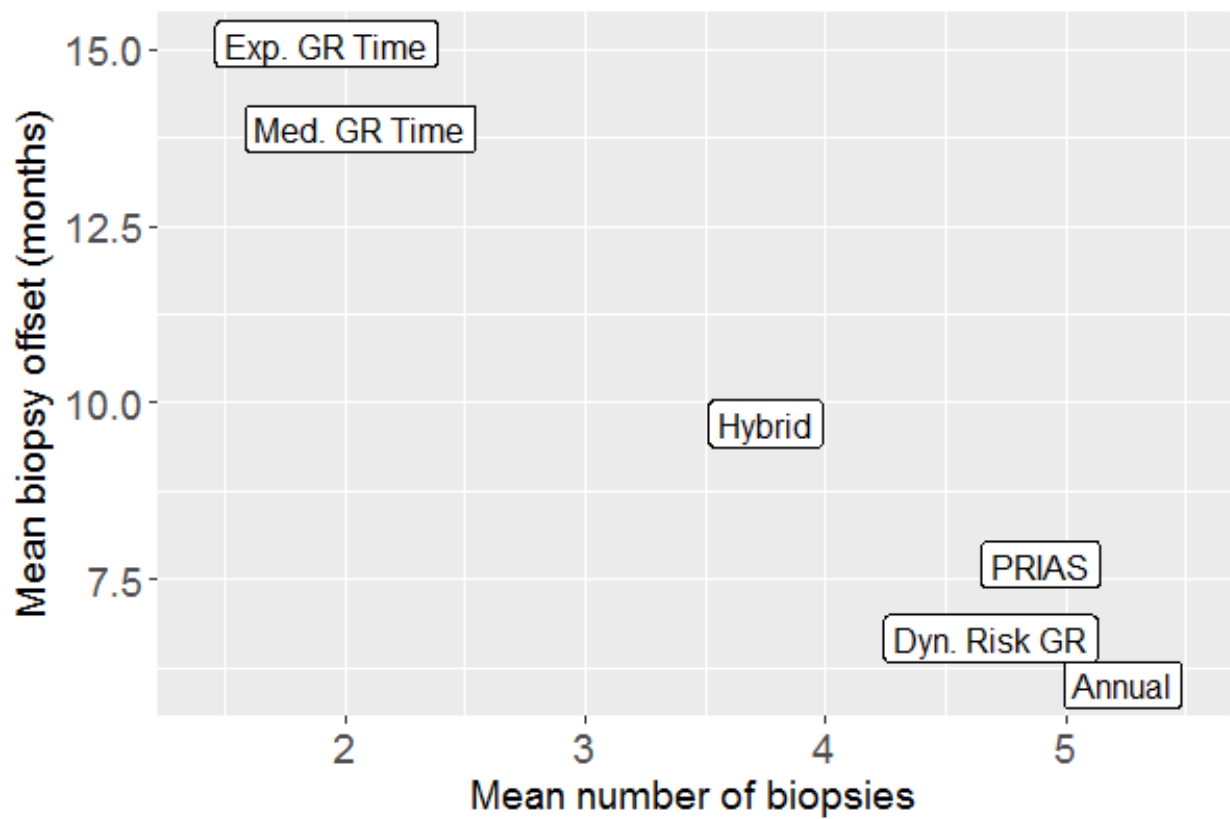
Figure 3. Estimated mean number of biopsies and mean offset (months) for the 6 schedules, using all 124781 patients. Method names are abbreviated for better readability.
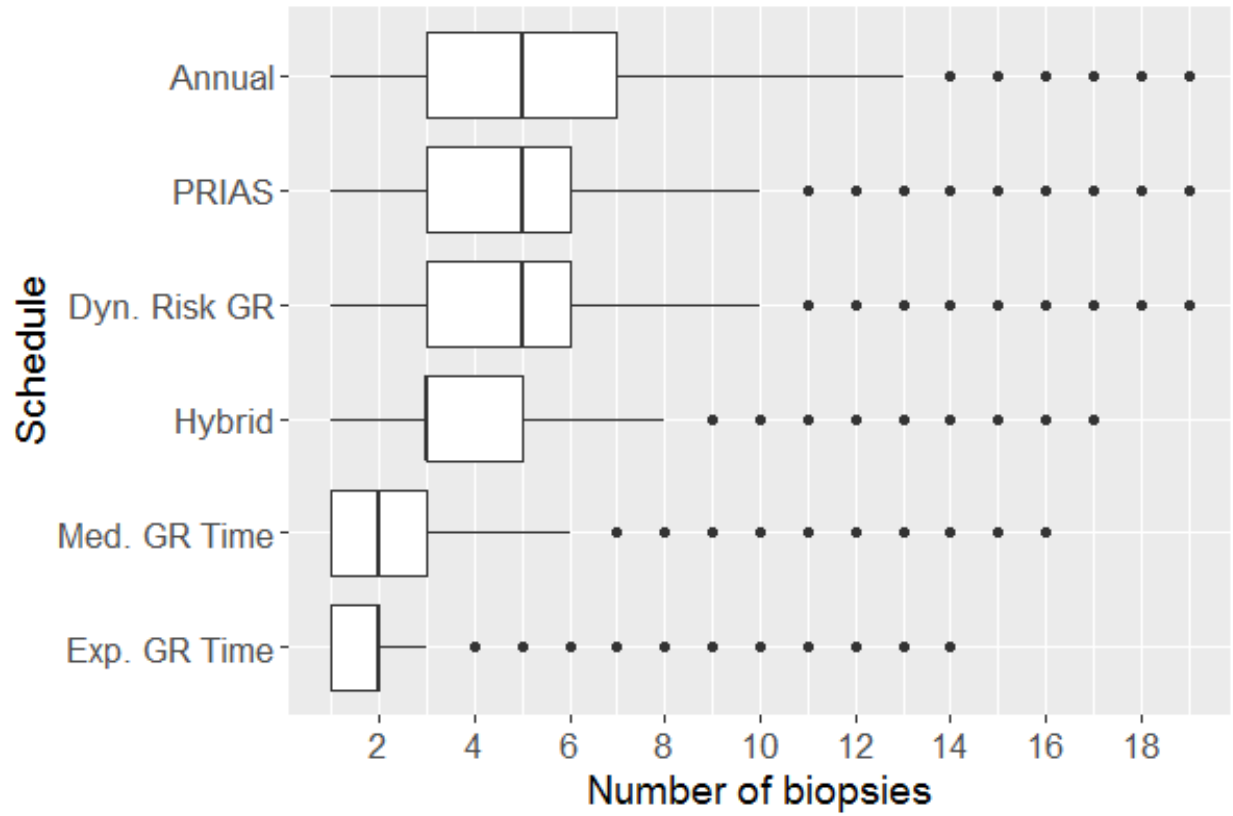
Figure 4. Boxplot showing variation in number of biopsies conducted by different methods, using all simulated patients.
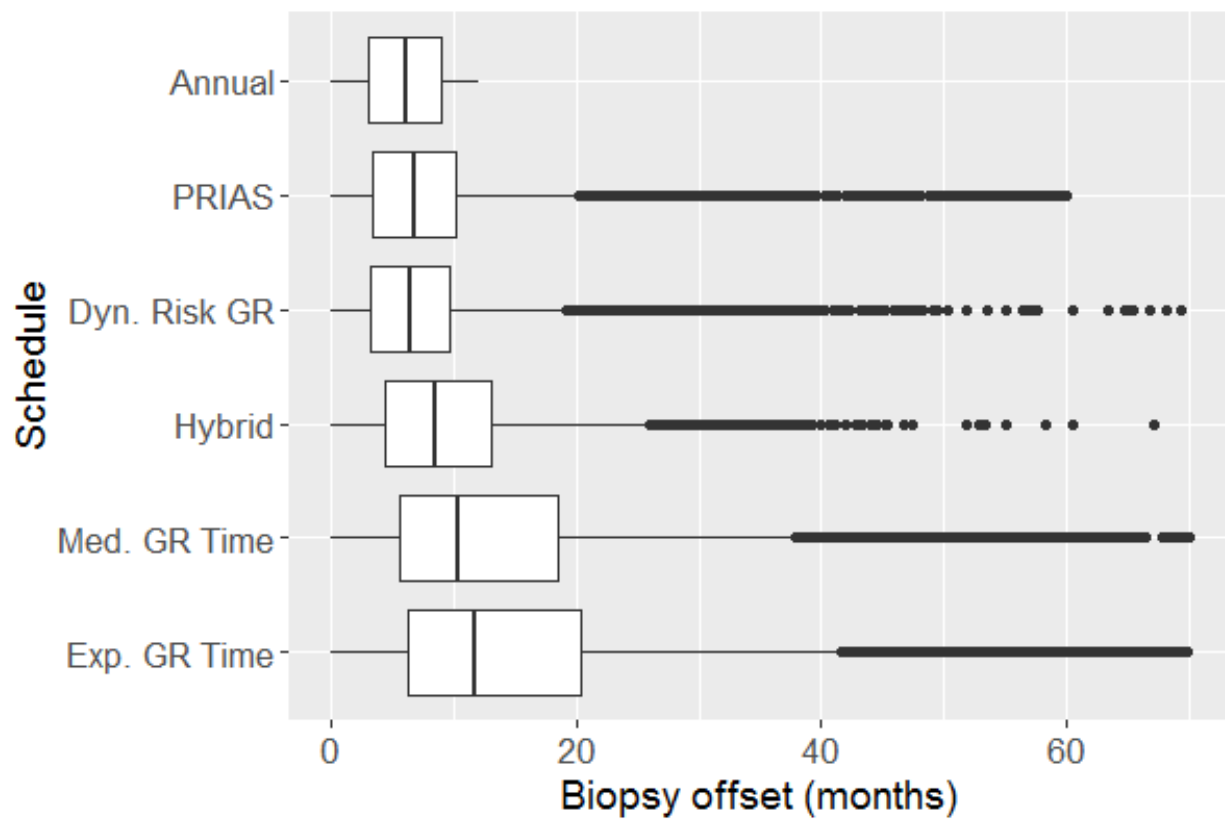
Figure 5. Boxplot showing variation in biopsy offset (months) for different methods, using all simulated patients. X-axis is trimmed at 70 months for visual clarity.

Table 1

Estimated mean and standard deviation of the number of biopsies and offset (months). Method names are abbreviated for consistency with Figure 3.

a) All subgroups: 125000 patients				
Schedule	$E(N_j^{bS})$	$E(O_j^S)$	SD$[N_j^{bS}]$	SD$[O_j^S]$
Annual	5.24	6.01	2.53	3.46
PRIAS	4.90	7.71	2.36	6.31
Exp. GR time	1.92	15.08	1.19	12.11
Med. GR time	2.06	13.88	1.41	11.80
Dyn. risk GR	4.69	6.66	2.19	4.38
Hybrid	3.75	9.70	1.71	7.25

b) Subgroup G_1: 41557 patients				
Schedule	$E(N_j^{bS})$	$E(O_j^S)$	SD$[N_j^{bS}]$	SD$[O_j^S]$
Annual	4.32	6.02	3.13	3.44
PRIAS	4.07	7.44	2.88	6.11
Exp. GR time	1.72	21.65	1.47	14.75
Med. GR time	1.84	20.66	1.76	14.62
Dyn. risk GR	3.85	6.75	2.69	4.44
Hybrid	3.25	10.25	2.16	8.07

c) Subgroup G_2: 41496 patients				
Schedule	$E(N_j^{bS})$	$E(O_j^S)$	SD$[N_j^{bS}]$	SD$[O_j^S]$
Annual	5.18	5.98	2.13	3.47
PRIAS	4.85	7.70	2.00	6.29
Exp. GR time	1.77	13.54	0.98	9.83
Med. GR time	1.89	12.33	1.16	9.44
Dyn. risk GR	4.63	6.66	1.82	4.37
Hybrid	3.68	10.32	1.37	7.45

d) Subgroup G_3: 41947 patients				
Schedule	$E(N_j^{bS})$	$E(O_j^S)$	SD$[N_j^{bS}]$	SD$[O_j^S]$
Annual	6.20	6.02	1.76	3.46
PRIAS	5.76	7.98	1.71	6.51
Exp. GR time	2.27	10.09	0.99	7.47
Med. GR time	2.45	8.70	1.15	6.32
Dyn. risk GR	5.58	6.58	1.56	4.33
Hybrid	4.32	8.55	1.26	5.91